

Accepted Manuscript

Fast regeneration of activated carbons saturated with textile dyes: Textural, thermal and dielectric characterization

Gabriela Durán-Jiménez, Lee A. Stevens, Genevieve R. Hodgins, Jacob Uguna, John Ryan, Eleanor R. Binner, John P. Robinson

PII: S1385-8947(19)31159-3
DOI: <https://doi.org/10.1016/j.cej.2019.05.135>
Reference: CEJ 21774

To appear in: *Chemical Engineering Journal*

Received Date: 26 March 2019
Revised Date: 18 May 2019
Accepted Date: 20 May 2019

Please cite this article as: G. Durán-Jiménez, L.A. Stevens, G.R. Hodgins, J. Uguna, J. Ryan, E.R. Binner, J.P. Robinson, Fast regeneration of activated carbons saturated with textile dyes: Textural, thermal and dielectric characterization, *Chemical Engineering Journal* (2019), doi: <https://doi.org/10.1016/j.cej.2019.05.135>

This is a PDF file of an unedited manuscript that has been accepted for publication. As a service to our customers we are providing this early version of the manuscript. The manuscript will undergo copyediting, typesetting, and review of the resulting proof before it is published in its final form. Please note that during the production process errors may be discovered which could affect the content, and all legal disclaimers that apply to the journal pertain.



Fast regeneration of activated carbons saturated with textile dyes:

Textural, thermal and dielectric characterization

Gabriela Durán-Jiménez, Lee A. Stevens, Genevieve R. Hodgins, Jacob Uguna, John Ryan,

Eleanor R. Binner, John P. Robinson*.

Low Carbon Energy and Resources Technologies Research Group, Faculty of Engineering, University of Nottingham, University Park, Nottingham, NG7 2RD, United Kingdom

Abstract

This study presents an investigation for comparing the regeneration process of two activated carbons saturated with Basic Blue 9 (BB9) and Acid Blue 93 (AB93) using conventional (250-500 °C) and microwave heating (100-300W). The effect of the textile dye used on the regeneration performance was analyzed by determining their dielectric properties using the perturbation cavity method from 20 to 600 °C and by TG/DTG analysis. The efficacy of the regenerated carbons was investigated by their physical properties characterized by pore structural analysis using N₂ adsorption isotherms. Results showed only 3 min are required by microwaves to achieve similar textural parameters obtained by conventional heating at 190 min. The results indicate that the adsorbate plays a determining role on the regeneration efficiency as results of their interaction with the adsorbent, being easily regenerated when AB93 is the adsorbate. The adsorption capacity of microwave regenerated samples for AB93 and BB9 was 192-240 and 154-175 mg/g, respectively. Additionally, the equilibrium isotherms were simulated using the Langmuir and Freundlich isotherms models and the results suggest the textile dye removal is achieved on multilayer adsorption.

*Corresponding author. E-mail: john.robinson@nottingham.ac.uk (John Robinson)

1. Introduction

Dye consumption in the textile industry is currently in excess of 10,000 tonnes per year [1], and this poses a major environmental challenge due to the large amounts of water required for the dyeing process. Textile wastewater is rich in salts, organic compounds, dyes and surfactants that are used to make clothes resistant to chemical and biological agents [2]. The release of dyes into the ecosystem has been recognized as a serious issue worldwide as many of these compounds are carcinogenic, mutagenic, bio-accumulative and persistent, causing a threat to human and environmental health [3, 4]. Many different techniques are already applied to treat industrial textile effluents, however adsorption is recognised as one of the most competitive processes because it is a cheap and simple method for removing different types of pollutants from water [5, 6].

Due to its low cost, porosity, well-developed internal surface area and high adsorption capacity, activated carbon (AC) is one of the most common adsorbents used in air and water treatment to adsorb organic contaminants [7-9]. Activated carbons have a finite capacity, so when its saturation adsorption capacity is reached (i.e. the material is 'spent'), these materials become hazardous residues which are incinerated or disposed of in landfills. From an environmental and sustainability standpoint the regeneration of spent adsorbents is a more attractive alternative. Several methods have been proposed to regenerate activated carbons, including electrochemical, microbiological, chemical and thermal regeneration [10-13].

Previous studies have shown that regeneration conditions and the heating method can impact on the structure of the activated carbon. Thermal regeneration is conventionally carried out in rotary kilns or tube furnaces under mildly oxidizing conditions (usually carbon dioxide and steam) [14, 15]. During the process, heat transfer takes place from the gas to the spent carbon in sequential steps of drying, pyrolysis and gasification [16]. The process is conduction-limited, meaning that high temperature and/or long residence times are required to achieve

the energy transfer necessary to regenerate the spent carbon. Consequently conventional process are both time and energy consuming and result in a loss of adsorption capacity due to deterioration of the pore structure after successive heating and cooling cycles [17]. Further drawbacks include attrition, burn-off and wash-out during thermal regeneration [18].

Microwave heating has been considered as an alternative to regenerate activated carbons due to its capability to heat volumetrically, overcoming the heat transfer limitations that underpin the disadvantages of conventional heating. Compared with conventional heating, microwave heating offers higher heating rates, greater control, heating selectivity, compact equipment and potential energy savings [19, 20]. Previous studies have demonstrated activated carbon can be effectively heated by microwaves since delocalized π electrons within the activated carbon allow for high levels of microwave absorbance and fast heating rates [21, 22].

The use of microwave heating for regeneration of adsorbents has been investigated since the 1980's [23], and in recent years several review papers have published on this topic [24-27]. Despite the number of previous studies, very few provide a robust comparison with conventional heating. Such a comparison requires performance information at multiple temperatures for conventional heating, multiple power/energy levels for microwave heating and knowledge of the dielectric properties of the system components.

Pi et al. [28] reported better cycling desulfurization performance of microwave-regenerated activated coke than that of conventional thermal regenerated activated coke. Caliskan et al., [29] investigated the regeneration of promethazine loaded activated carbon, and showed that microwave regeneration had a lower efficiency compared to conventional process. Their results were attributed to an enhanced cracking of the pollutant caused by direct interaction between the adsorbate and the microwaves. Ania et al. investigated the regeneration of activated carbon saturated with phenol [17, 20] and salicylic acid [30]. Their results showed that the regeneration time was considerably shorter compared to conventional heating and the

microwave regeneration process preserved the porous structure compared with conventional regeneration. Fayaz et al.[31] studied the regeneration of activated carbon loaded with n-dodecane and their results demonstrated improvements in desorption efficiency and claimed that the energy requirements with the microwave process were around 5% of the energy needed conventionally. Mao et al. [32] showed that microwave desorption can regenerate activated carbon adsorbed of toluene and acetone more efficiently than conventional regeneration, and concluded that microwave regeneration was achieved up to 6 times faster than conventional regeneration.

The microwave regeneration process is affected by the properties of the adsorbent, but also the quantity, location and properties of the adsorbed species (adsorbates). Microwave energy dissipates within an adsorbent and/or adsorbate as heat according to its dielectric properties, particularly the loss tangent. Roh et al. [33] introduced the importance of dielectric properties for microwave regeneration for the removal of NO_x using HZSM-5. They showed that pure zeolite does not absorb microwave energy, and consequently it had to be modified to increase its microwave susceptibility [33]. Further improvements in microwave regeneration were reported by modifying the zeolite with cations such as Li^+ , K^+ , Na^+ and Ba^{2+} [34]. In this case it was found that cations with different electronegativity can modify the surface charge, cation mobility and subsequently the dielectric properties.

Dielectric properties of materials are highly dependent on the microwave frequency, temperature, water content and density [21, 35-39]. Despite the importance of dielectric properties in understanding microwave heating behaviour, to date only one study has measured these properties for adsorbent/adsorbate systems and temperatures that are representative for a thermal desorption process [40]. The lack of dielectric characterization in previous work prevents the necessary understanding of microwave regeneration phenomena, and prevents a meaningful comparison with conventional regeneration methodologies.

The objective of this study was to understand the impact of adsorbate properties (i.e., Basic Blue 9 and Acid Blue 93) on the regeneration of two commercial activated carbons using both microwave heating and conventional heating. The efficiency of the microwave regeneration process and its impact on the characteristics of the adsorbent and adsorptive performance were studied using thermal, dielectric and textural characterization. The results were compared with those of thermal regeneration conducted under conventional electric heating under equivalent operating conditions. Our results show that the microwave regeneration process was faster than the conventional thermal process by more than two orders of magnitude, and for the first time identifies the significance of the adsorbate properties on the regeneration process.

2. Material and methods

2.1 Activated carbons and textile dyes

The two commercial activated carbon selected in this study were obtained from steam activation of coconut shells (CC) and bituminous charcoal (Ch), and were obtained from Filtracarb® CPL and Norit® respectively. Both activated carbons were washed using hot distilled water (80 °C) to remove impurities until reaching neutral pH, then were dried at 110 °C for 24 h and sieved to obtain a particle size of ~1 mm. The target textile dyes considered for the adsorption studies, Basic Blue 9 (BB9) and Acid Blue 93 (AB93) were chosen due to the large difference in molecular size and purchased from Sigma Aldrich at reagent grade and used without further purification. Their properties are shown in Table 1.

2.2 Thermal and dielectric characterization of activated carbons and textile dyes

The dielectric properties of the carbons and textile dyes were obtained at 2.45 GHz using the cavity perturbation technique [15]. Approximately 0.1 g of sample was placed in a quartz

tube (3 mm ID) supported on porous glass fibre. The tube was purged with nitrogen flowing at 5 mL/min to avoid oxidation at high temperatures. The sample was heated to the target temperature by a furnace located above the cavity. A step-motor rapidly moved the sample into the cavity to make the measurement, then returned the sample to the furnace. The reported dielectric constant and loss factor values were based on triplicate measurements in a temperature range from 20 and 600 °C.

The thermogravimetric analysis of the dyes, virgin and saturated carbons was performed in a SDT Q600 apparatus from TA instruments. The thermograms were obtained from room temperature up to 900 °C using a heating rate of 5 °C/min under a nitrogen flow rate of 25 mL/min.

2.3 Textural analysis and pH_{pzc}

The textural properties of the samples were calculated from the sorption isotherms of nitrogen at -196 °C using a Micromeritics® ASAP 2420 apparatus from 0.00005 to 0.99 relative pressure (P/P_0). The surface area was calculated using the Brunauer–Emmett–Teller (BET) theory [41], based on adsorption data in the range of 0.01–0.1 P/P_0 to give positive BET ‘C’ parameters. The narrow micropore, micropore and total pore volumes and size distributions were determined by Non-Local Density Functional Theory (NLDFT) on carbon slit pores by combining a CO₂ adsorption isotherm at 0 °C to a N₂ adsorption isotherm beginning at 0.0005 P/P_0 using Microactive Software V5.0.

Point of zero charge was estimated following a previously reported methodology [42]. In this case, 0.120 g of each carbon was mixed for 24 h with 40 mL of 0.01 M NaCl at different initial pH values. pH was adjusted by adding NaOH or HCl. The final pH was measured after 24 h.

2.4 Dye adsorption studies

All dye solutions were prepared using distilled water. Three types of adsorption tests were performed. The first was carried out for the virgin carbons and regenerated samples (see Table 2), using an initial dye concentration of 1500 mg/L. Adsorption tests were conducted in batch systems at 30 °C, stirring at 150 rpm with 0.02 g of AC in 10 mL of dye solution. After 48 h the adsorbents were decanted from the dye solution and the liquid remaining was analyzed by UV–Vis spectrophotometry employing a Hach DR-5000 spectrophotometer. Adsorption equilibrium was determined using kinetic data shown in Fig. S1 (Supporting information). The dye concentration at equilibrium was calculated from the calibration curve, which was obtained at the maximum wavelength for each dye (see Table 1). The amount of dye adsorbed was calculated using a mass balance relationship given by Eq. (1):

$$q = \left(\frac{C_0 - C_e}{W} \right) V \quad \text{Eq. (1)}$$

Where C_0 and C_e are the initial and equilibrium dye concentrations (mg/L), V is the volume of the solution (L) and W is the weight of the adsorbent used (g).

The second type of adsorption test was carried out to establish the dye adsorption isotherms. These experiments were limited to the virgin and selected microwave and conventional regenerated carbons, which showed higher adsorption capacity in the preliminary adsorption experiments. In these cases an initial dye concentration ranging from 50 to 1500 mg/L was used, with temperature, stirring speed and adsorbent loading as described above.

Finally, a comparative study of the adsorption on selected regenerated samples after several adsorption-regeneration cycles was carried out using an initial concentration of 1500 mg/L. Triplicates for all adsorption tests were carried out and standard deviations were below 5% of average values.

2.5 Regeneration of spent activated carbons

Regeneration experiments on saturated carbons were carried out using samples processed as described in section 2.4. Before regeneration tests were carried out the saturated activated carbons were separated from the dye solution and dried at 100 °C for 24 h to remove free water.

2.5.1 Microwave regeneration

Microwave (MW) regeneration was carried out in a CEM Discover® SP single mode cavity at 2.45 GHz according to the conditions described in Table 2. 2 g of spent carbon was used in each regeneration experiment. The spent carbon was placed into a quartz tube under a nitrogen atmosphere at 200 mL/min, 1 bar and centered within the microwave cavity. The surface temperature of the sample was measured with an infrared temperature sensor from the open top of the cavity immediately after each treatment; the resulting temperature values are also reported in Table 2. It should be noted that the temperature values are an indication of a single-point temperature reached by the sample surface during the experiments, however a representative average temperature measurement is not possible due to the volumetric and instantaneous nature of the microwave heating process. This is confirmed by the lack of correlation between temperature and power/time in Table 2. The yield is defined as the weight of regenerated activated carbon per weight of spent activated carbon utilized for regeneration of the previous cycle. The adsorption-regeneration process was carried out for selected carbons for several cycles. The samples were labeled according to w - x - y - z where w represents the regeneration method (MW), x refers to the carbon (CC or Ch), y describes the dye used to saturate the carbon (BB9 or AB93) and z represents the power and time used for microwave regeneration (See Table 2).

2.5.2 Conventional regeneration

Conventional regeneration (CF) experiments were performed in a tubular furnace (Carbolite CTF 12165/550). Experiments were carried out using a heating rate of 3 °C/min to a target temperature, at which the sample was held for a further 30 minutes. All the experiments were conducted in nitrogen flowing at 200 mL/min. The samples were labelled as w - x - y - z where w represents the regeneration method (CF), x refers to the carbon (CC or Ch), y describes the dye used to saturate the carbon (BB9 or AB93) and z represents the temperature used for regeneration.

2.6 Isotherm modelling

Adsorption data modeling was carried out on the experimental isotherms. Langmuir model assumes that the adsorption occurs on a monolayer where the active sites are identical and energetically equivalent. This model is represented by:

$$q_e = \frac{Q_M B C_e}{1 + B C_e} \quad \text{Eq. (2)}$$

where q_e and C_e are the dye uptake (mg/g) and concentration (mg/L) at equilibrium, Q_M is the theoretical monolayer adsorption capacity (mg/g), and B (L/mg) represents the Langmuir equilibrium constant, indicating the solid surface affinity and ability. Both Q_M and B are obtained from data correlation. Alternatively, Freundlich isotherm adsorption equation is semi-empirical model, assuming that the adsorption process occurs on the heterogeneous surface and is defined as:

$$q_e = K C_e^{1/N} \quad \text{Eq. (3)}$$

where K and N are parameters characteristic of the adsorbent-sorbate system, which can be determined from nonlinear fitting of Eq. 4.

Parameters of isotherms models were determined via global optimization approach using a stochastic method (i.e. simulated annealing) and following the objective function [43]:

$$F_{obj} = \frac{ndat}{i=1} \sum_{i=1}^{ndat} \left(\frac{q_e^{exp} - q_e^{calc}}{q_e^{exp}} \right)_i^2 \quad \text{Eq. (4)}$$

where q_{exp} and q_{calc} are the experimental and predicted adsorption capacities, respectively. The mean absolute percentage deviation (E_{abs}) between calculated and experimental dye adsorption capacities:

$$E_{abs} = \frac{100}{ndat} \sum_{i=1}^{ndat} \left| \frac{q_e^{exp} - q_e^{calc}}{q_e^{exp}} \right|_i \quad \text{Eq. (5)}$$

3. Results and discussion

3.1 Thermal analysis of dyes and spent carbons

The thermal profiles of the dyes, virgin and spent AC's are shown in Fig. 1. It can be seen that significant differences exist between the dyes, virgin and spent carbons. From room temperature to 110 °C the dye compounds exhibit a weight loss of 15% (BB9) and 7% (AB93). The virgin carbons show a weight loss <3%, whilst losses up to 7% are observed for the saturated carbons. In this temperature region the weight losses are primarily due to moisture. At temperatures up to 300 °C a weight loss of 29% is shown for BB9, which can also be observed as a sharp peak in derivative graph (Fig. 1 a). At 300 °C the AB93 dye showed a mass loss of 11%, followed by a sharp increase in the TG curve around 410 °C with a mass loss of 25%. This is likely due to decomposition of the dye compound [44]. Both dyes experience significant weight loss from 500-800 °C, however AB93 has a larger and more complex structure than BB9, and Fig. 1(b) shows that this compound is more stable at lower temperatures.

Fig. 1 also illustrates the differences between the virgin and spent carbons. A significant difference is observed for Ch and Ch-BB9, with weight loss of 1.7 and 6.7% at 400 °C (Fig.

1. c). The weight loss of saturated carbons observed in Fig. 1 could involve two separate mechanisms as temperature increases: (a) thermal desorption of volatile organics initially adsorbed on the activated carbon and (b) decomposition of the dye on the adsorbent surface via thermal cracking, leaving behind a charred residue within the pore structure [45].

3.2 Dielectric properties of dyes and carbon adsorbents

The interaction between the electric field component of the microwave and the sample was characterized by the dielectric properties. The loss tangent ($\tan\delta$) gives a measure of the relative ability of a material to heat, and is calculated from the dielectric constant (ϵ') and the loss factor (ϵ''), as follow:

$$\tan\delta = \frac{\epsilon''}{\epsilon'} \quad \text{Eq. (6)}$$

Details of the method used to calculate the loss tangent are reported by Adam *et al.* [46]. The microwave absorption capability of dyes BB9 and AB93, and virgin activated carbons CC and Ch are shown in Fig. 2. The results indicate the dielectric properties of both dyes and activated carbons are significantly influenced by the temperature. As can be observed in Fig, 2(a) at room temperature the loss tangent of both dyes are comparable at around 0.04, significantly below the carbons which exhibit a loss tangent of around 0.15 (Fig. 2 (b)). At room temperature the carbons will heat selectively, with neither dye absorbing appreciable amounts of microwave energy. BB9 exhibits a loss tangent decrease in the 100-175 °C temperature range, which corresponds to the weight loss observed in Fig. 1(a).

At 300 °C both dyes show a peak in loss tangent, which is likely due to the remaining molecules after thermal decomposition being more receptive to microwaves [45]. Activated carbons are known to be strong microwave absorbers [47] and this is confirmed by the loss tangent data in Fig. 2 (b). The microwave absorption capability of AB93 is poor compared with the activated carbons, this means that carbons saturated with AB93 will absorb

microwave energy in the first instance, with the dye being heated as a secondary effect due to conventional heat transfer within the carbon. BB9 behaves differently, and in this case both the dye and the carbon will absorb microwave energy at temperatures from 100-175 °C. At higher temperatures it is the carbon that absorbs microwaves, with higher adsorbate temperatures obtained through secondary heat transfer. The key finding from Fig 2 (a-b) is that selective heating of the dye will not take place when activated carbons are used as adsorbents, but rather the carbons themselves have a tendency to be selectively heated. Desorption/decomposition of the adsorbates occurs due to the temperatures attained, which occurs primarily due to conductive heat transfer from the higher temperature regions within the activated carbon.

3.3 Regeneration of spent activated carbon by microwave and conventional heating

Table 2 shows the experimental conditions for the regeneration of coconut activated carbon saturated with BB9 (CC-BB9) and AB93 (CC-AB93), and charcoal activated carbon saturated with BB9 (Ch-BB9) and AB93 (Ch-AB93). Given the data from each condition of regeneration, it was found for the 1st regeneration cycle the yields from the microwave heating are comparable to those obtained by conventional heating. In general, the yields observed in microwave regeneration tests were higher for the samples obtained at the lowest power and shortest time. This suggests that the energy absorbed (absorbed power x time) is a critical parameter, with higher energy levels giving higher internal temperatures that could decompose both the dye and also the carbon matrix.

The observed yield of microwave regenerated samples was slightly higher for carbons saturated with AB93 (94-98%) compared to BB9 (92-95%). Samples regenerated at 500 °C by conventional heating showed lower yields (~92%) than those obtained at 250 °C (98%).

The surface temperature of the microwave regenerated samples was measured at a single point by an infrared sensor from the open top of the cavity immediately after each experiment, and the resulting temperatures are reported in Table 2. The recorded temperatures give a very crude estimate of the temperature reached by the sample surface during the experiments. Microwave heating is volumetric, so the electric field penetrates within the sample and decays in magnitude with sample depth and loss factor. [48, 49]. The results shown in Fig. 2 confirm that activated carbons are high loss tangent materials, so the penetration depth is low and heat dissipation is heterogeneous. In addition, there are convective heat losses from the outside of the sample (where the measurement is taken). Consequently the surface temperature values reported in Table 2 cannot be deemed to be representative of the temperature throughout the whole sample, and are likely to underestimate with respect to the real temperatures reached beyond the sample surface.

3.4 Effect of regeneration conditions on dye uptake and textural properties of regenerated carbons

3.4.1 Coconut (CC) regenerated samples

The adsorption uptake onto virgin and regenerated coconut carbons as function of the regeneration condition is shown in Fig. 3(a), which indicates that uptake is highly dependent on regeneration conditions. Fig. 3(a) illustrates that dye adsorption decreases in regenerated samples compared to the virgin CC activated carbon, and it was found the better performance was achieved for the regenerated samples at 500 °C for 11300 sec in conventional heating (CF-CC-2), and at 200 W and 180 sec in microwave (MW-CC-4). For BB9 the adsorption capacity of CC-virgin, MW-CC-4 and CF-CC-2 is 232, 154 and 220 mg/g, respectively. These results are in agreement with the textural parameters reported in Table 3 and Fig. 4,

where a clear correlation is observed between BB9 removal and specific surface area (S_{BET}) and also the micropore volume.

It is evident that BB9 removal is favored when regenerating using conventional heating (CF-CC-2). Compared to the virgin carbon, the CF-CC-2 recovered almost all of its initial surface area and micropore volume (See Table 3). The S_{BET} of virgin CC activated carbon is 1131 m^2/g which decreased to 679 m^2/g after being loaded with BB9 (Fig. S2 and Table 1S, supporting information). The surface area of CF-CC-2 is 1087 m^2/g , while the surface area of the microwave regenerated sample (MW-CC-4) and area is 960 m^2/g . Despite BB9 removal in MW-CC-4 being lower than CF-CC-2, it is important to note that a significant degree of regeneration was obtained by microwave heating at 180 seconds, whereas the conventional regeneration took two orders of magnitude longer at 11300 seconds.

AB93 exhibited a lower uptake than BB9 with the virgin CC samples, however all but one of the microwave regeneration conditions resulted in higher levels of subsequent AB93 uptake compared with BB9. With conventional regeneration at 500 °C the AB93 uptake was considerably lower than BB9 under the same conditions. Table 3 shows that the regenerated carbons MW-CC-AB93-(1-6) are mainly microporous materials, along with the virgin carbon. The S_{BET} of virgin CC activated carbon decreased from 1131 m^2/g to 1037 m^2/g after being loaded with AB93, and interestingly the textural parameters were slightly improved after the regeneration, reaching S_{BET} values up to 1188 m^2/g .

3.4.2 Charcoal (Ch) regenerated samples

The removal of BB9 and AB93 onto virgin and charcoal regenerated samples (Ch) is presented in Fig. 3 (b). Similar to the coconut-derived carbon, it was found that AB93 removal is more favorable than the removal of BB9 during regeneration of the charcoal-derived carbon. According to the results shown in Table 4, and Fig. S2 (b), Ch carbon is both

micro- and mesoporous. The removal of BB9 during Ch regeneration was proportional to the S_{BET} and the micropore volume. For the microwave regenerated samples the highest uptake for BB9 was 175 mg/g obtained for MW-Ch-5, which corresponds to a S_{BET} of 733 m^2/g . Conventional regeneration (CF-Ch-2) also gave high levels of BB9 uptake (192 mg/g), which correlated with an increase in the surface area (790 m^2/g).

When AB93 was used there was no clear correlation between uptake after regeneration and the textural parameters of either of the carbons (See Fig. 4). AB93 uptake was generally higher for Ch regenerated samples compared with CC, which can be attributed to the higher mesopore volume in the Charcoal-derived carbon. Comparing microwave and conventional regenerated samples it was found that for MW-Ch-AB93 the mesopore volume was 24.1, compared to 18.6% for CF-Ch-2. This was in agreement with AB93 uptake, which was 240 mg/g for the microwave regenerated sample and 220 mg/g for conventional regeneration.

Micropores are less than 2 nm in diameter, and provide activated carbons with the majority of their surface area. Mesopores are defined between 2 and 50 nm, and their contribution to the total surface area of activated carbons is usually small compared to micropores. However, the results of this study show that mesopores play an important role in the adsorption of large molecules (i.e. AB93), which are too large to access the micropores.

A linear relationship between BB9 uptake and micropore volume was observed for both CC and Ch regenerated carbons. This compound has a smaller molecular size (0.8 nm) [50] than AB93 (1.93 nm) and hence can access the large micropores [51]. BB9 is therefore more challenging to remove than AB93 during the regeneration process as it is present within the micropore matrix, whereas AB93 is contained predominantly on the surface of the carbons as a result of electrostatic attraction between SO_3^- groups in the anionic dye and the positively charged groups on the surface of the carbon. Table 1S confirms that the micropore volume of

both carbons is reduced significantly when saturated with BB9, but reduced to a much lesser extent when AB93 is used.

3.5 Adsorption isotherms on selected carbons and modelling

In addition to molecular size the adsorption and desorption process is influenced by the chemistry of the dye and the surface chemistry of the adsorbent, adsorption isotherms were obtained for virgin and selected regenerated samples to assess the adsorption mechanism for each dye, as shown in Fig. 5 & 6. Adsorption models of Langmuir and Freundlich were used to predict the sorption mechanism, surface properties and affinity of the carbon adsorbent toward the adsorption process [52]. The fitting results are also presented in Fig. 4 & 5.

The isotherms of CC- virgin and CF-CC-2 are very similar for BB9, while MW-CC-4 showed a lower adsorption capacity. The Freundlich model correlated best with all isotherms for BB9, ($R^2 = 0.99$ and $E_{\text{abs}} = 2.6\%$). Indicating that the lower adsorption capacity for MW-CC-4 is due to a reduction in surface area and micropore volume after regeneration (See Fig. 5 (a) and Table 5).

The pore size distribution shows the sharpest peaks occurred at pore diameter between 0.3 and 1 nm and the majority of the pores fall into the range of micropores with the average pore size of 1.53 nm. Fig. 7 shows that the pore size distribution does not appear to be affected by the regeneration method, however the total pore volume decreased in MW-CC-BB9-4 by ~16% from the original CC- virgin. The corresponding decrease for the conventional regeneration CF-CC-BB9-2 was just 2%. This implies that a fraction of the absorbed BB9 did not evolve from the carbon during the microwave regeneration, with the dye remaining within the pore network of the carbon. The regeneration process can involve thermal desorption of volatiles, or thermal decomposition [44]. The latter typically results in the evolution of volatile breakdown products, accompanied by a residual and non-volatile solid

char. The carbon porosity following regeneration will depend on the extent of adsorbate removal and also the residual decomposed matter that will form deposits and block the pores [17].

The AB93 uptake onto Coconut virgin and regenerated samples is illustrated in Fig. 5 (b). Non- correlation between the removal of AB93 and the micropore and mesoporous volume was found (See Fig. 4). Results indicate the AB93 removal can be as result of adsorption on multilayers onto the external surface of the carbon and can be governed by mechanisms of i.e., π - π dispersion, hydrogen bond formation, the electronic mechanism of complex formation [53]. This results are in agreement with the reported in Table 5 and Fig. S3 (supporting information). The point of zero charge (pHpzc) for virgin Coconut and Charcoal is 9.9 and 8.89, respectively. As the adsorption experiments were carried out at pH \sim 7, both materials have a positive surface charge since pH < pHpzc. A strong electrostatic interaction is expected between the positive surface of the carbons and the anionic AB93 ($-\text{SO}_3^-$ groups). The opposite effect is expected for the cationic dye (BB9), with adsorption governed by intraparticle diffusion due to its small molecular size.

The adsorption isotherms of BB9 onto virgin and regenerated Charcoal samples is shown in Fig. 6 (a). MW-Ch-5 and CF-Ch-2 regenerated samples showed comparable BB9 adsorption performance, which corresponds to similarities in their textural properties. S_{BET} values were 733 and 790 m^2/g and mesopore volumes were 25% and 24% in MW-Ch-5 and CF-Ch-2, respectively. The increase on BB9 adsorption capacity from 175 to 192 mg/g for the microwave and conventional regenerated samples (Fig. 6 (a)), could be associated to the increase in the micropore volume for the conventional sample (See Table 4). The pore size distribution shows the pore width of regenerated Ch decreases, indicating that obstruction of the larger pores may have occurred due to deposition of residue from dye decomposition (Fig. 8).

BB9 adsorption isotherms for both conventional and microwave regenerated Charcoal are better represented by the Freundlich model than the Langmuir model ($R^2 = 0.90; 0.95$), however the virgin material is better represented by the Langmuir isotherm (See Table 6). This implies that the morphology of MW-Ch-5 and CF-Ch-2 samples could be more heterogeneous after the regeneration process. This is in agreement with SEM images obtained for both samples (See. Fig. S4, supporting information) [40].

The uptake of AB93 onto virgin and regenerated Ch is presented in Fig. 6 (b). At low concentrations ($C_{eq} < 100$ mg/L) the AB93 dye adsorbs with a monolayer coverage on the carbon surface until all the available sites are saturated, showing a classical profile up to this point. At increasing dye concentration an inflexion point in the isotherm can be observed, indicating that multilayer adsorption is favoured within this concentration range [54]. The Freundlich model ($N > 1$) reveals the favourability and capacity of the adsorption process (See Table 6). From the two isotherm models, due to higher R^2 values and the lower E_{abs} the Freundlich model was deemed to be the better fit, indicating that the adsorption of AB93 on the regenerated samples takes place via multilayer adsorption on a heterogeneous surface [55].

The regeneration of Ch samples saturated with AB93 takes place more readily than when saturated with BB9, irrespective of the regeneration method. For example, Fig. 3 shows that the adsorption capacity of AB93 following microwave and conventional regeneration is equivalent to the virgin Ch, whereas when BB9 was used the original capacity was never reached under any of the regeneration conditions tested. This is due primarily to the larger size of the AB93 molecule which preferentially adsorbs on the surface of the carbon since it is less able to access the narrow micropores.

3.6 Reusability and dye uptake after regeneration cycles

Fig. 9 shows the adsorption capacities for BB9 and AB93 on MW-CC-4 and MW-Ch-5 carbons after successive regeneration cycles, with S_{BET} also plotted. Textural parameters are detailed in Table 7. BB9 uptake decreased progressively over 5 adsorption-regeneration cycles, which is consistent with a decline in specific surface area. In the regeneration process the deterioration of the pore structure becomes particularly apparent after 4 cycles, where the surface area of MW-CC-BB9-4 dropped 32% from the virgin CC and the adsorption capacity decreased from 261 to 27 mg/g. Similar results were observed for BB9 and Ch, where after 4 cycles S_{BET} decreased from 1023 to 513 m²/g and adsorption capacity from 235 to 39 mg/g.

Samples loaded with AB93 showed more resilience after 4 regeneration cycles. For MW-CC-AB93-4 samples S_{BET} was practically unchanged after 4 cycles, however a deterioration in adsorption capacity was observed after the second cycle. By the 4th cycle the AB93 uptake had decreased to 50 mg/g from an initial value of 201 mg/g for the virgin carbon. This result is in agreement with the hypothesis described before, where it is evident that the AB93 is adsorbed mainly in the larger pores. The charcoal regenerated sample (MW-Ch-AB93-5) showed similar behavior, with a marked decrease in capacity after the 3rd regeneration cycle that correlates with a reduction in the mesopore volume. For both dyes and carbons it is apparent therefore that since the dyes are removed by thermal decomposition then the remaining solid residue acts to inhibit further dye uptake. For AB93, which adsorbs primarily within mesopores the effect becomes particularly noticeable at the third adsorption-regeneration cycle, however the smaller BB9 molecule that adsorbs within micropores suffers a noticeable reduction in capacity even after one cycle.

3.7 Heating mechanisms on regeneration process

The temperatures attained within the carbon bed during microwave heating cannot be measured accurately, however, the results shown in Table 2 and Fig. 5 & 6 are consistent with the dielectric and thermal properties shown in Fig. 1 and Fig. 2. Temperatures in excess of 200 °C are required before any appreciable removal of the dye and or decomposed products takes place. The dielectric property measurements show that BB9 absorbs microwaves up to 175 °C, and the temperature range that corresponds to dye decomposition, the dyes themselves are effectively microwave-transparent, and it is the carbons that act as the dominant microwave-absorbing phase [32].

The dominant mechanism by which the dyes are heated during microwave regeneration is therefore due to conventional heat-transfer, from the high temperature surroundings of the activated carbon that is itself heated volumetrically. The heating mechanism is very similar to conventional heating, the only difference being that the carbon is heated by a hot gas rather than by an electric field. It is not surprising therefore that the microwave and conventional regeneration processes produce the same end result, given that the heating mechanism is in fact the same. However, the volumetric nature of the heating that occurs during microwave regeneration means that the carbon bed can be heated much faster than by conventional means, which explains the significant reduction in regeneration time between the two techniques.

4. Conclusions

This study has shown that the regeneration of activated carbons is primarily dependent on the physical characteristics of the adsorbate and the pore structure of the carbons, rather than the heating method. Conventional thermal regeneration and microwave regeneration were both able to regenerate two adsorbents loaded with two different organic dyes, with little difference in regeneration efficiency. Dye decomposition occurred with both regeneration

methods, and ultimately led to a decrease in adsorption capacity over multiple regeneration cycles. Dielectric property measurements confirmed that no selective heating of the adsorbed species takes place when activated carbons are used as the adsorbent, however the microwave heating process was able to regenerate the spent adsorbents over two order of magnitude faster than the conventional heating process.

It is possible that microwave regeneration could offer further benefits if changes are made to the adsorbent/adsorbate system and to the process conditions:

1. If the adsorbates themselves are microwave absorbent within the process temperature range. In this case selective heating of the adsorbates will occur, and heat-transfer will no longer take place via conduction from the activated carbon.
2. If the spent carbons are not dried prior to regeneration. In this case steam will be produced in-situ from the water that is present within the carbon, which has been previously demonstrated to significantly increase mass-transfer within fixed-bed processing systems.

Further work will investigate the two options above, and will aim to further define the technical and economic benefits of microwave regeneration compared to conventional heating.

5. Acknowledgments

Authors are grateful to the Consejo Nacional de Ciencia y Tecnologia (CONACyT), Mexico for the grant 389535.

References

1. Rahmani, M., M. Kaykhaii, and M. Sasani, *Application of Taguchi L16 design method for comparative study of ability of 3A zeolite in removal of Rhodamine B and Malachite green from environmental water samples*. Spectrochimica Acta Part A: Molecular and Biomolecular Spectroscopy, 2018. **188**: p. 164-169.

2. Punzi, M., et al., *Combined anaerobic–ozonation process for treatment of textile wastewater: removal of acute toxicity and mutagenicity*. Journal of hazardous materials, 2015. **292**: p. 52-60.
3. Shanker, U., M. Rani, and V. Jassal, *Degradation of hazardous organic dyes in water by nanomaterials*. Environmental Chemistry Letters, 2017. **15**(4): p. 623-642.
4. Khamparia, S. and D.K. Jaspal, *Adsorption in combination with ozonation for the treatment of textile waste water: a critical review*. Frontiers of Environmental Science & Engineering, 2017. **11**(1): p. 8.
5. Kyzas, G.Z., et al., *Synthesis and adsorption application of succinyl-grafted chitosan for the simultaneous removal of zinc and cationic dye from binary hazardous mixtures*. Chemical Engineering Journal, 2015. **259**: p. 438-448.
6. Angin, D., *Utilization of activated carbon produced from fruit juice industry solid waste for the adsorption of Yellow 18 from aqueous solutions*. Bioresource technology, 2014. **168**: p. 259-266.
7. Waheed ul Hasan, S. and F.N. Ani, *Review of Limiting Issues in Industrialization and Scale-up of Microwave-Assisted Activated Carbon Production*. Industrial & Engineering Chemistry Research, 2014. **53**(31): p. 12185-12191.
8. Pezoti, O., et al., *NaOH-activated carbon of high surface area produced from guava seeds as a high-efficiency adsorbent for amoxicillin removal: kinetic, isotherm and thermodynamic studies*. Chemical Engineering Journal, 2016. **288**: p. 778-788.
9. Saleh, T.A., M. Tuzen, and A. Sari, *Polyethylenimine modified activated carbon as novel magnetic adsorbent for the removal of uranium from aqueous solution*. Chemical Engineering Research and Design, 2017. **117**: p. 218-227.
10. Hou, P., et al., *Electrochemical regeneration of polypyrrole-tailored activated carbons that have removed sulfate*. Carbon, 2014. **79**: p. 46-57.
11. Sodha, K., S.C. Panchani, and K. Nath, *Feasibility study of microbial regeneration of spent activated carbon sorbed with phenol using mixed bacterial culture*. 2013.
12. Li, Q., Y. Qi, and C. Gao, *Chemical regeneration of spent powdered activated carbon used in decolorization of sodium salicylate for the pharmaceutical industry*. Journal of cleaner production, 2015. **86**: p. 424-431.
13. Berenguer, R., et al., *Comparison among chemical, thermal, and electrochemical regeneration of phenol-saturated activated carbon*. Energy & Fuels, 2010. **24**(6): p. 3366-3372.
14. Xin-hui, D., C. Srinivasakannan, and L. Jin-sheng, *Process optimization of thermal regeneration of spent coal based activated carbon using steam and application to methylene blue dye adsorption*. Journal of the Taiwan Institute of chemical engineers, 2014. **45**(4): p. 1618-1627.
15. Maroto-Valer, M.M., et al., *Thermal regeneration of activated carbons saturated with ortho- and meta-chlorophenols*. Thermochimica Acta, 2006. **444**(2): p. 148-156.
16. Foo, K., *Effect of microwave regeneration on the textural network, surface chemistry and adsorptive property of the agricultural waste based activated carbons*. Process Safety and Environmental Protection, 2018. **116**: p. 461-467.
17. Ania, C., et al., *Microwave-induced regeneration of activated carbons polluted with phenol. A comparison with conventional thermal regeneration*. Carbon, 2004. **42**(7): p. 1383-1387.
18. Jeon, J.-K., et al., *Regeneration of field-spent activated carbon catalysts for low-temperature selective catalytic reduction of NO_x with NH₃*. Chemical engineering journal, 2011. **174**(1): p. 242-248.
19. Berenguer, R., et al., *Comparison among Chemical, Thermal, and Electrochemical Regeneration of Phenol-Saturated Activated Carbon*. Energy & Fuels, 2010. **24**(6): p. 3366-3372.

20. Ania, C., et al., *Effect of microwave and conventional regeneration on the microporous and mesoporous network and on the adsorptive capacity of activated carbons*. *Microporous and Mesoporous Materials*, 2005. **85**(1-2): p. 7-15.
21. Foo, K. and B. Hameed, *Microwave-assisted regeneration of activated carbon*. *Bioresource technology*, 2012. **119**: p. 234-240.
22. Hashisho, Z., et al., *Role of functional groups on the microwave attenuation and electric resistivity of activated carbon fiber cloth*. *Carbon*, 2009. **47**(7): p. 1814-1823.
23. Roussy, G., et al., *How microwaves dehydrate zeolites*. *The Journal of Physical Chemistry*, 1984. **88**(23): p. 5702-5708.
24. Yuen, F.K. and B. Hameed, *Recent developments in the preparation and regeneration of activated carbons by microwaves*. *Advances in colloid and interface science*, 2009. **149**(1-2): p. 19-27.
25. Jones, D.A., et al., *Microwave heating applications in environmental engineering—a review*. *Resources, conservation and recycling*, 2002. **34**(2): p. 75-90.
26. Haque, K.E., *Microwave energy for mineral treatment processes—a brief review*. *International journal of mineral processing*, 1999. **57**(1): p. 1-24.
27. Menéndez, J., et al., *Microwave heating processes involving carbon materials*. *Fuel Processing Technology*, 2010. **91**(1): p. 1-8.
28. Pi, X., et al., *Microwave irradiation induced high-efficiency regeneration for desulfurized activated coke: A comparative study with conventional thermal regeneration*. *Energy & Fuels*, 2017. **31**(9): p. 9693-9702.
29. Çalışkan, E., et al., *Low temperature regeneration of activated carbons using microwaves: Revising conventional wisdom*. *Journal of environmental management*, 2012. **102**: p. 134-140.
30. Ania, C., et al., *Microwave-assisted regeneration of activated carbons loaded with pharmaceuticals*. *Water research*, 2007. **41**(15): p. 3299-3306.
31. Fayaz, M., et al., *Using microwave heating to improve the desorption efficiency of high molecular weight VOC from beaded activated carbon*. *Environmental science & technology*, 2015. **49**(7): p. 4536-4542.
32. Mao, H., et al., *Constant power and constant temperature microwave regeneration of toluene and acetone loaded on microporous activated carbon from agricultural residue*. *Journal of Industrial and Engineering Chemistry*, 2015. **21**: p. 516-525.
33. Roh, H.-S., Y.-K. Park, and S.-E. Park, *Abatement of NO_x through the Adsorption-Desorption Cycle Assisted by Microwave Irradiation*. *Journal of Industrial and Engineering Chemistry*, 2001. **7**(5): p. 326-331.
34. Shariaty, P., et al., *Effect of ETS-10 ion exchange on its dielectric properties and adsorption/microwave regeneration*. *Separation and Purification Technology*, 2017. **179**: p. 420-427.
35. Sun, Y., et al., *Regeneration of activated carbon saturated with chloramphenicol by microwave and ultraviolet irradiation*. *Chemical Engineering Journal*, 2017. **320**: p. 264-270.
36. Cheng, S., et al., *Microwave-assisted regeneration of spent activated carbon from paracetamol wastewater plant using response surface methodology*. *Desalination and Water Treatment*, 2016. **57**(40): p. 18981-18991.
37. Jiang, Y., et al., *Simultaneous biogas purification and CO₂ capture by vacuum swing adsorption using zeolite NaUSY*. *Chemical Engineering Journal*, 2018. **334**: p. 2593-2602.
38. Fang, C. and P.M. Lai, *Microwave regeneration of spent powder activated carbon*. *Chemical engineering communications*, 1996. **147**(1): p. 17-27.
39. Liu, X., G. Yu, and W. Han, *Granular activated carbon adsorption and microwave regeneration for the treatment of 2, 4, 5-trichlorobiphenyl in simulated soil-washing solution*. *Journal of hazardous materials*, 2007. **147**(3): p. 746-751.

40. Lin, G., et al., *High temperature dielectric properties of spent adsorbent with zinc sulfate by cavity perturbation technique*. Journal of hazardous materials, 2017. **330**: p. 36-45.
41. Thommes, M., et al., *Physisorption of gases, with special reference to the evaluation of surface area and pore size distribution (IUPAC Technical Report)*. Pure and Applied Chemistry, 2015. **87**(9-10): p. 1051-1069.
42. Durán-Jiménez, G., et al., *Study of the adsorption-desorption of Cu²⁺, Cd²⁺ and Zn²⁺ in single and binary aqueous solutions using oxygenated carbons prepared by Microwave Technology*. Journal of Molecular Liquids, 2016. **220**: p. 855-864.
43. Duran-Jimenez, G., et al., *Adsorption of dyes with different molecular properties on activated carbons prepared from lignocellulosic wastes by Taguchi method*. Microporous and Mesoporous Materials, 2014. **199**: p. 99-107.
44. Wang, J., et al., *Regeneration of carbon nanotubes exhausted with dye reactive red 3BS using microwave irradiation*. Journal of hazardous materials, 2010. **178**(1-3): p. 1125-1127.
45. Suzuki, M., et al., *Study of thermal regeneration of spent activated carbons: thermogravimetric measurement of various single component organics loaded on activated carbons*. Chemical Engineering Science, 1978. **33**(3): p. 271-279.
46. Adam, M., et al., *Microwave synthesis of carbon onions in fractal aggregates using heavy oil as a precursor*. Carbon, 2018. **138**: p. 427-435.
47. Shkal, F., et al., *Microwave Characterization of Activated Carbons*. Journal of Computer and Communications, 2017. **6**(01): p. 112.
48. Tripathi, M., et al., *Effect of temperature on dielectric properties and penetration depth of oil palm shell (OPS) and OPS char synthesized by microwave pyrolysis of OPS*. Fuel, 2015. **153**: p. 257-266.
49. Jimenez, G.D., et al., *New insights into microwave pyrolysis of biomass: Preparation of carbon-based products from pecan nutshells and their application in wastewater treatment*. Journal of Analytical and Applied Pyrolysis, 2017. **124**: p. 113-121.
50. Hernández-Montoya, V., et al., *Competitive adsorption of dyes and heavy metals on zeolitic structures*. Journal of environmental management, 2013. **116**: p. 213-221.
51. San Miguel, G., S. Lambert, and N. Graham, *The regeneration of field-spent granular-activated carbons*. Water Research, 2001. **35**(11): p. 2740-2748.
52. Yao, S., et al., *Removal of Pb (II) from water by the activated carbon modified by nitric acid under microwave heating*. Journal of colloid and interface science, 2016. **463**: p. 118-127.
53. Guo, Y. and E. Du, *The effects of thermal regeneration conditions and inorganic compounds on the characteristics of activated carbon used in power plant*. Energy Procedia, 2012. **17**: p. 444-449.
54. Scheufele, F.B., et al., *Monolayer–multilayer adsorption phenomenological model: kinetics, equilibrium and thermodynamics*. Chemical Engineering Journal, 2016. **284**: p. 1328-1341.
55. Liu, L., et al., *Adsorption removal of dyes from single and binary solutions using a cellulose-based bioadsorbent*. ACS Sustainable Chemistry & Engineering, 2015. **3**(3): p. 432-442.

Captions

Figure 1. TG and DTG curves of textile dyes BB9, CC virgin & CC loaded with BB9 (a), AB93, CC virgin & CC loaded with AB93 (b) BB9, Ch virgin & Ch loaded with BB9 (c) and AB93 Ch virgin & Ch loaded (d) with AB93 in nitrogen atmosphere.

Figure 2. Loss tangent of textile dyes BB9 & AB93 (a) and CC & Ch activated carbons.

Figure 3. Adsorption capacity of BB9 and AB93 in CC (a) and Ch (b) activated carbons. Experimental conditions: 2 g/L, $C_0 = 1500$ mg/L, 30 °C, 160 rpm, 48 h, one regeneration cycle.

Figure 4. Correlation of dye uptake onto CC and Ch regenerated activated carbons regarding to the S_{BET} , micropore volume (V_{micro}) and mesoporous volume (V_{mes}).

Figure 5. Adsorption isotherms and modelling of BB9 (a) and AB93 (b) employing the virgin and selected regenerated Coconut carbons. Experimental conditions: C_0 : 50–1500 mg/L, temperature: 30 °C, agitation: 150 rpm, mass to volume ratio: 2 g/L and equilibrium time 48 h.

Figure 6. Adsorption isotherms and modelling of BB9 (a) and AB93 (b) employing the virgin and selected regenerated Charcoal carbons. Experimental conditions: C_0 : 50–1500 mg/L, temperature: 30 °C, agitation: 150 rpm, mass to volume ratio: 2 g/L and equilibrium time 48 h.

Figure 7. N_2 and CO_2 combined adsorption isotherms at -196 (N_2) and 0 °C (CO_2) of the virgin and selected regenerated Coconut carbon samples with microwave and conventional heating.

Figure 8. N_2 and CO_2 combined adsorption isotherms at -196 (N_2) and 0 °C (CO_2) of the virgin and selected regenerated Charcoal carbon samples with microwave and conventional heating.

Figure 9. Adsorption capacity of virgin and regenerated carbons after several cycles (a) CC activated carbon regenerated using 200 W and 180 sec (MW-CC-4), (b) Ch activated carbon regenerated using 300 W and 90 sec (MW-Ch-5).

Fig. 1.

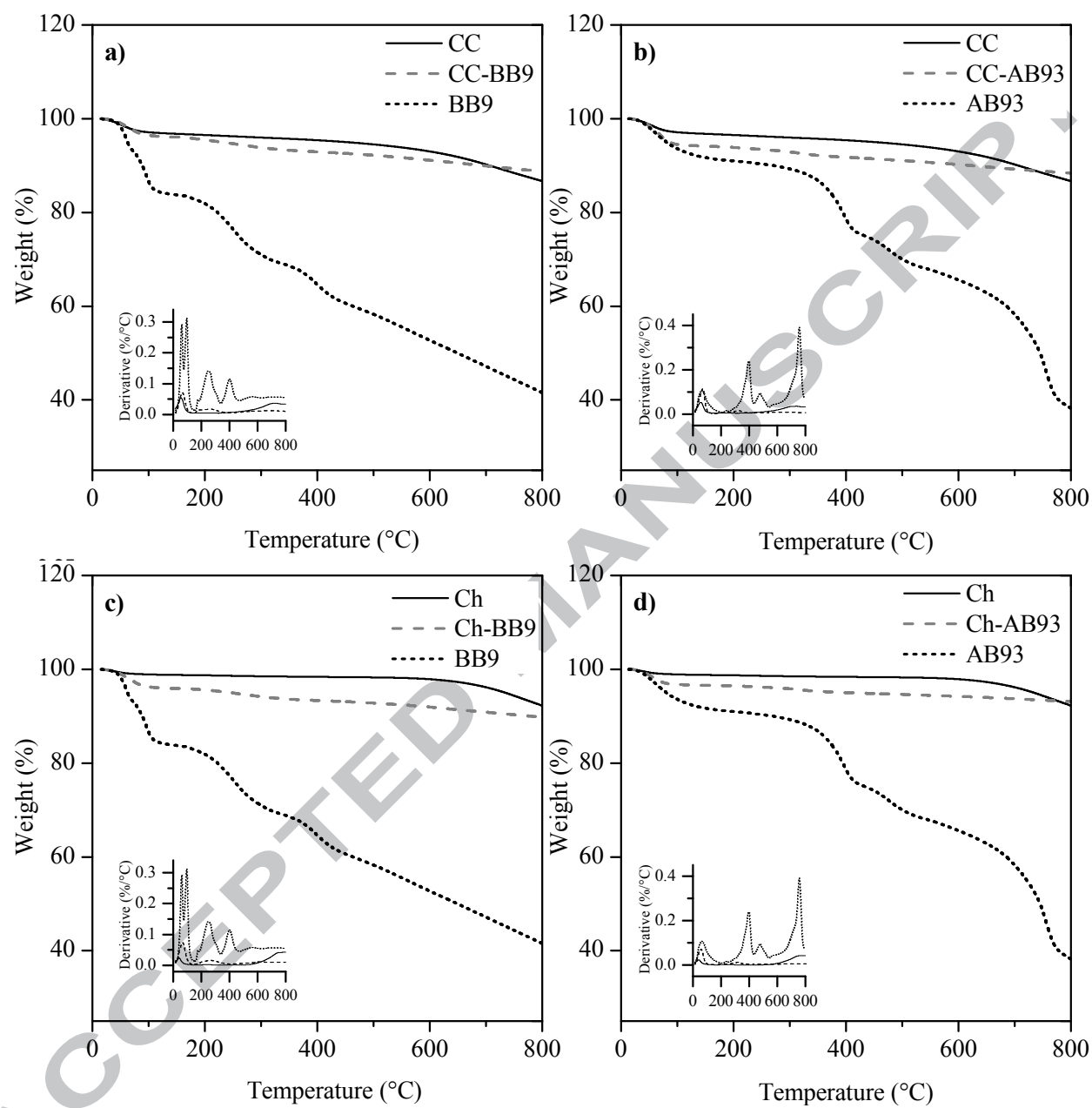


Fig. 2

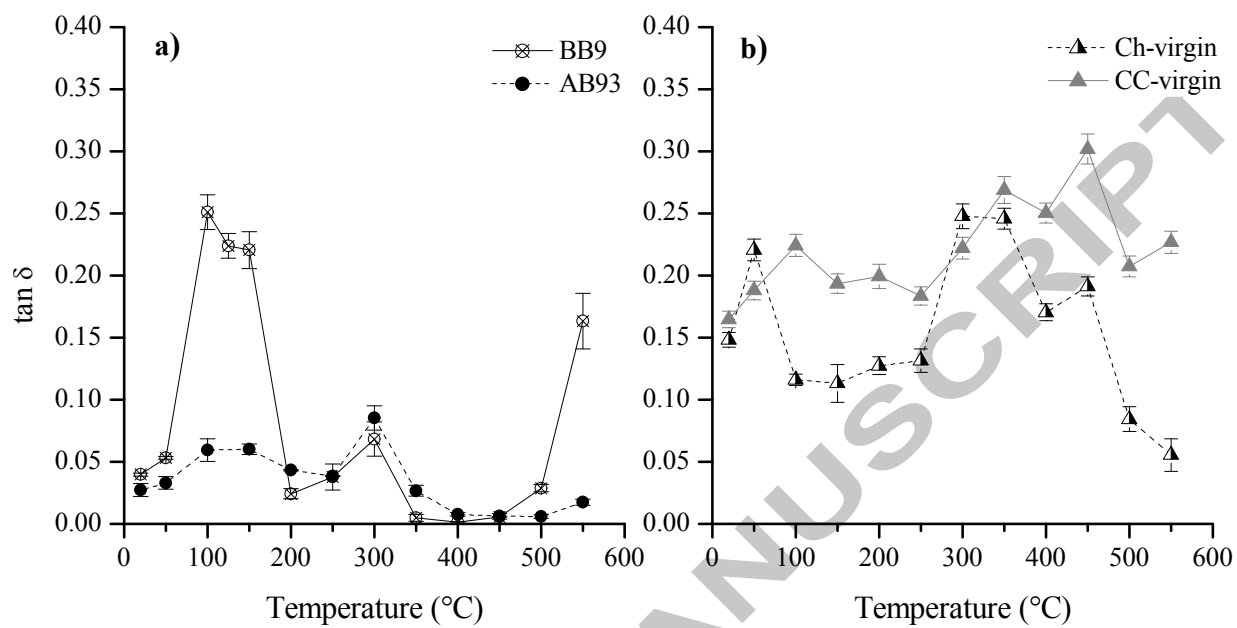


Fig. 3

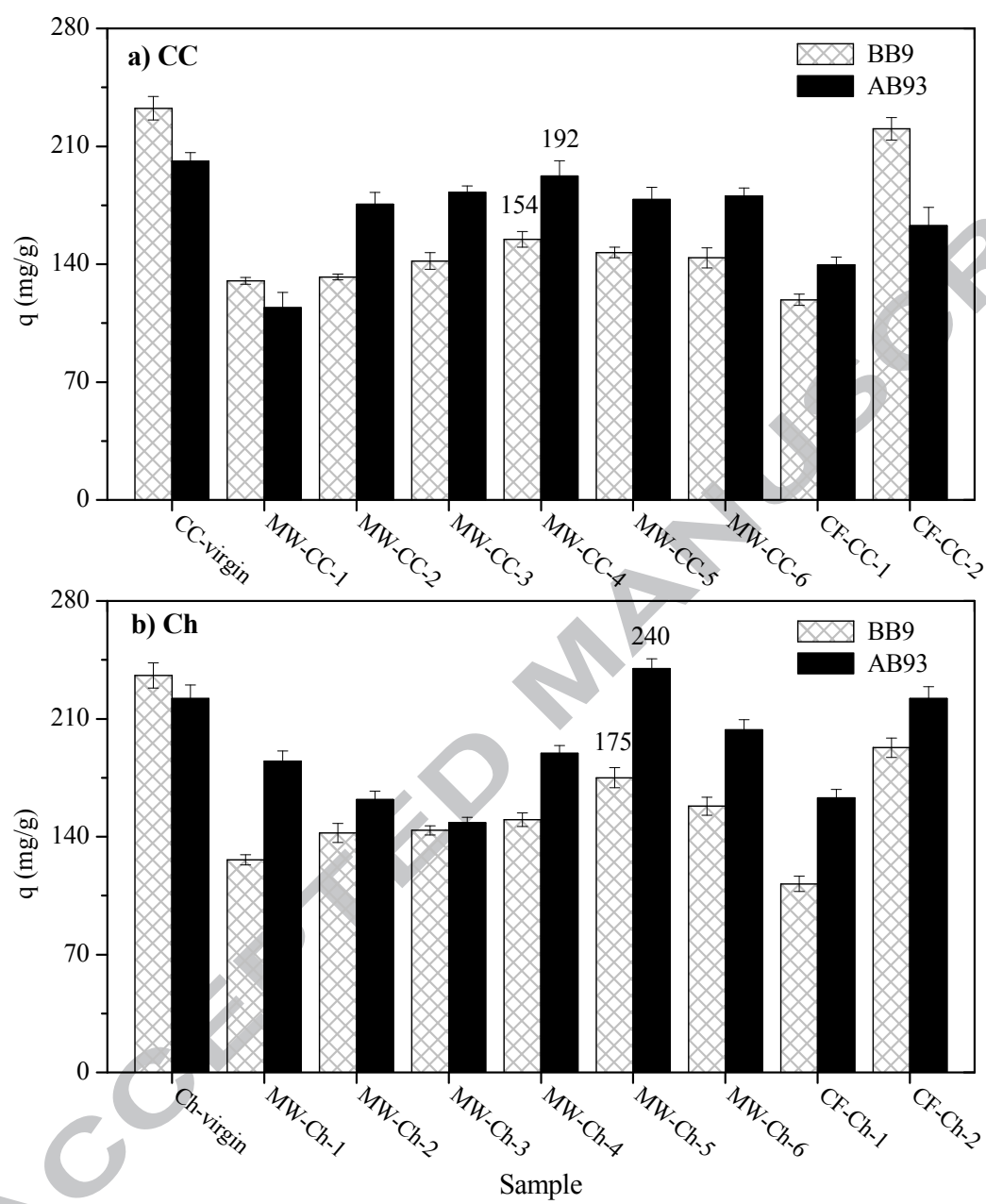


Fig. 4

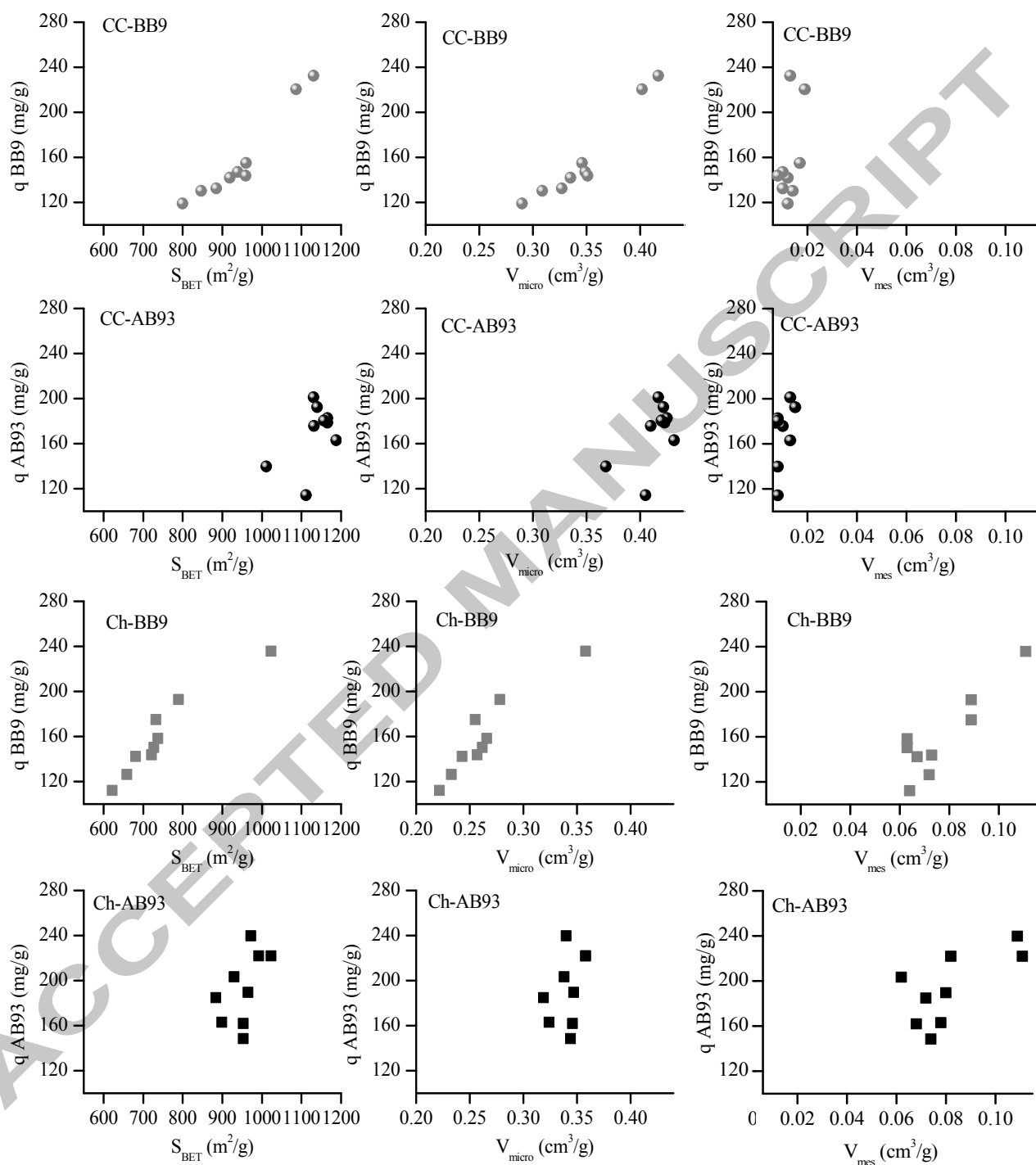


Fig. 5

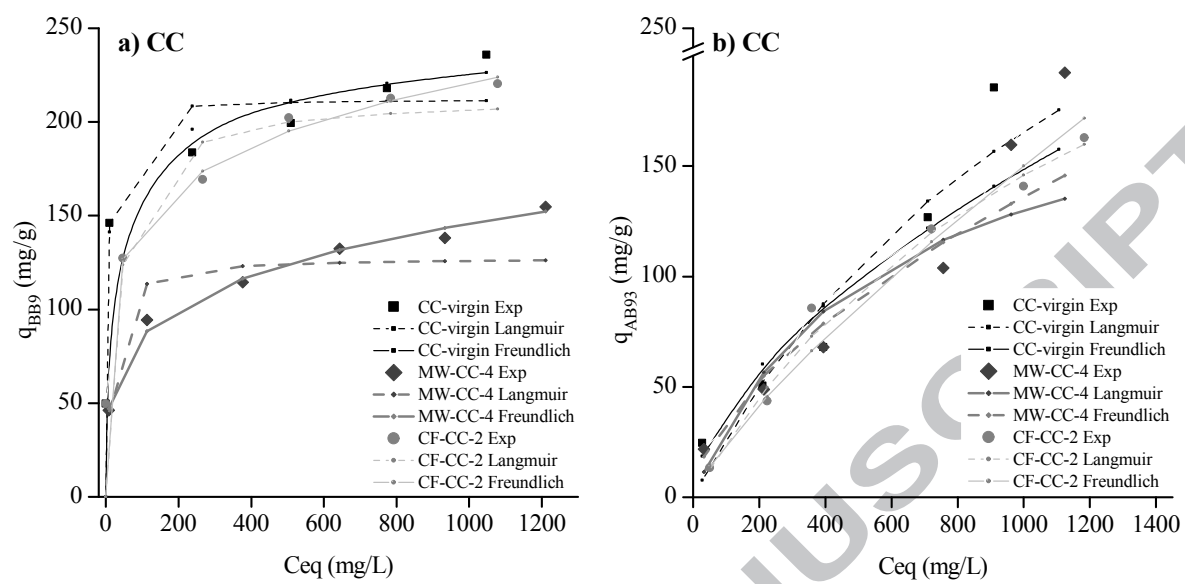


Fig. 6

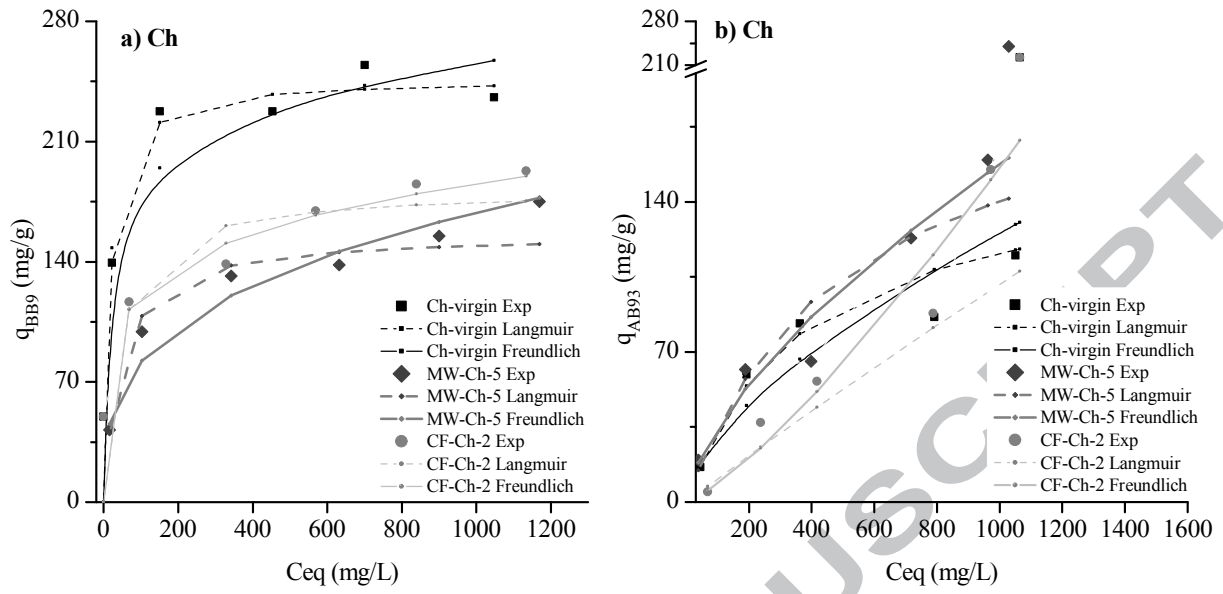


Fig. 7.

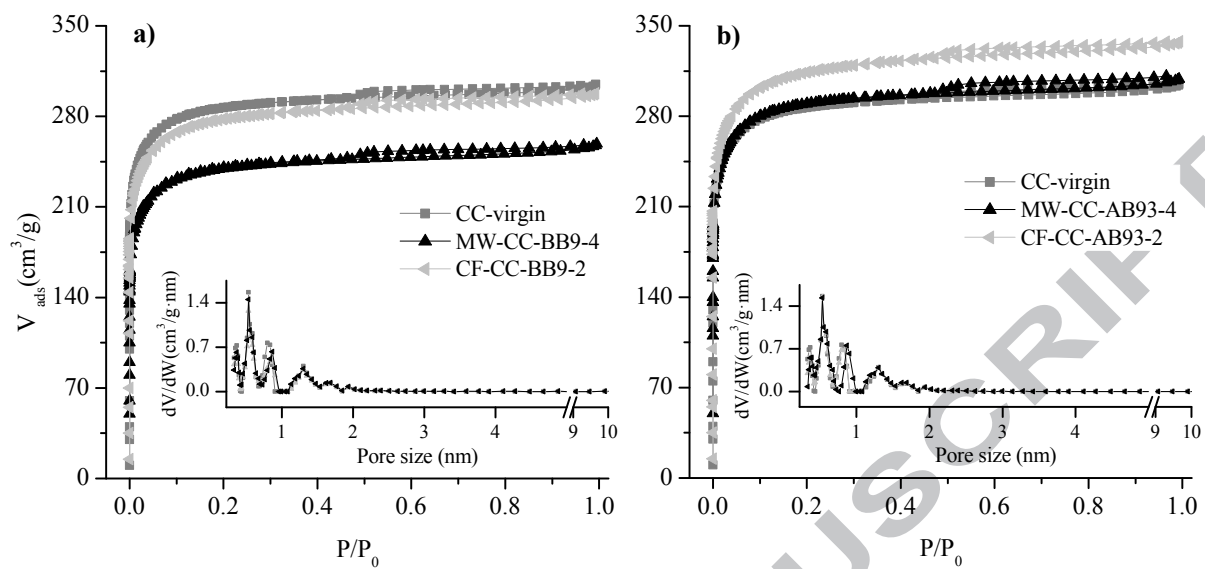


Fig. 8

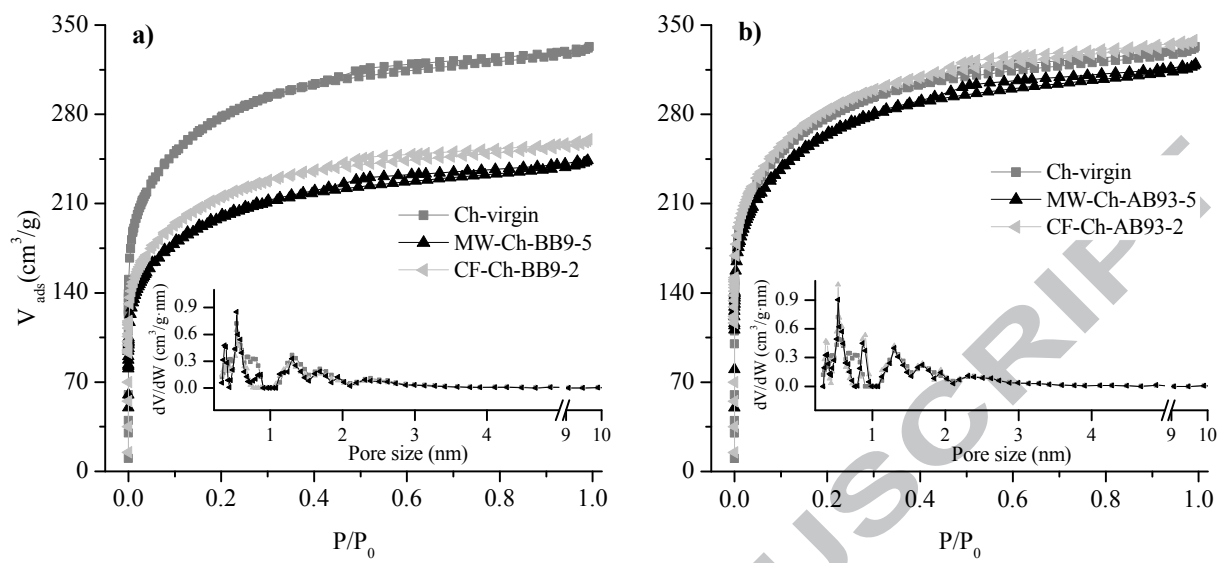


Fig. 9

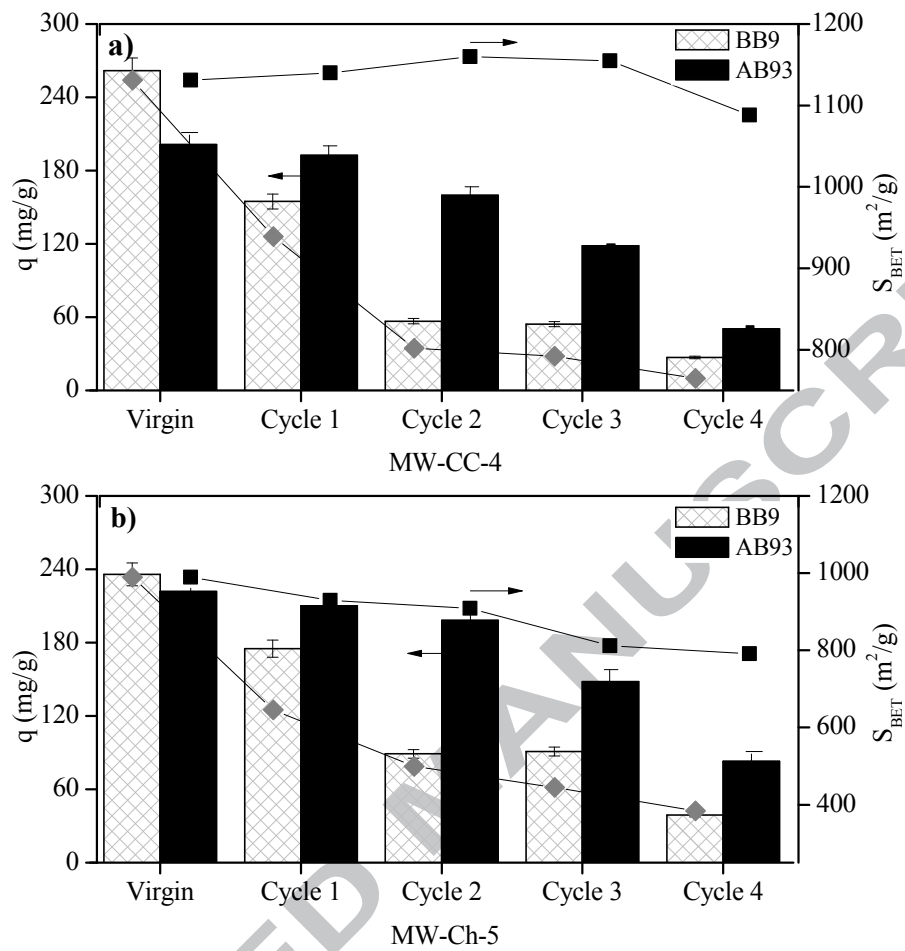


Table 1. Characteristics of the studied dyes

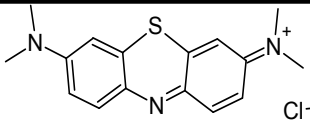
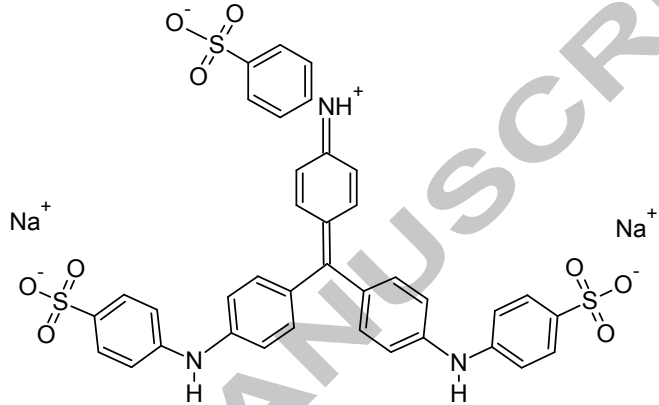
Generic name (code)	Mass (amu)/ Dye type	Structure	λ_{\max} (nm)
Basic Blue 9 (BB9)	319.8 Cationic	 $C_{16}H_{18}N_3SCl$	664
Acid Blue 93 (AB93)	799.8 Anionic	 $C_{37}H_{27}N_3Na_2O_9S_3$	604

Table 2. Experimental conditions of the 1st regeneration cycle of spent activated carbons and yields after each condition of regeneration.

	Sample	Power, W	*t, sec	^a T _{IR sensor} , °C	Yield, %	Sample	Power, W
MICROWAVE	MW-CC-BB9-1	100	90	253	95.2	MW-Ch-BB9-1	100
	MW-CC-BB9-2	100	180	278	94.5	MW-Ch-BB9-2	100
	MW-CC-BB9-3	200	90	286	93.2	MW-Ch-BB9-3	200
	MW-CC-BB9-4	200	180	305	93.1	MW-Ch-BB9-4	200
	MW-CC-BB9-5	300	90	294	92.8	MW-Ch-BB9-5	300
	MW-CC-BB9-6	300	180	315	92.3	MW-Ch-BB9-6	300
	MW-CC-AB93-1	100	90	335	96.7	MW-Ch-AB93-1	100
	MW-CC-AB93-2	100	180	341	96.4	MW-Ch-AB93-2	100
	MW-CC-AB93-3	200	90	365	95.8	MW-Ch-AB93-3	200
	MW-CC-AB93-4	200	180	324	95.1	MW-Ch-AB93-4	200
	MW-CC-AB93-5	300	90	372	93.9	MW-Ch-AB93-5	300
	MW-CC-AB93-6	300	180	381	94.1	MW-Ch-AB93-6	300

CONVENTIONAL	Sample	T _{regen} , °C	*t, sec		Yield, %	Sample	T _{regen} , °C
	CF-CC-BB9-1	250	6300	-	97.7	CF-Ch-BB9-1	250
	CF-CC-BB9-2	500	11300	-	92.0	CF-Ch-BB9-2	500
	CF-CC-AB93-1	250	6300	-	98.8	CF-Ch-AB93-1	250
	CF-CC-AB93-2	500	11300	-	91.4	CF-Ch-AB93-2	500

*Total processing time

^a Temperature measured with IR sensor after the microwave regeneration

Table 3. Textural parameters of virgin and regenerated coconut-derived carbons by microwave and conventional heating

	Sample	^a S _{BET} (m ² /g)	^b V _t (cm ³ /g)	^c V _{micro} (cm ³ /g)	^d V _{mes} (cm ³ /g)
MICROWAVE	CC virgin	1,131	0.431	0.417	0.013
	MW-CC-BB9-1	847	0.324	0.309	0.014
	MW-CC-BB9-2	885	0.339	0.327	0.010
	MW-CC-BB9-3	919	0.349	0.335	0.012
	MW-CC-BB9-4	960	0.364	0.346	0.017
	MW-CC-BB9-5	939	0.360	0.349	0.010
	MW-CC-BB9-6	959	0.361	0.351	0.008
	MW-CC-AB93-1	1,112	0.414	0.405	0.008
	MW-CC-AB93-2	1,132	0.421	0.410	0.010
	MW-CC-AB93-3	1,166	0.434	0.425	0.008
	MW-CC-AB93-4	1,140	0.439	0.422	0.015
	MW-CC-AB93-5	1,166	0.431	0.423	0.007
	MW-CC-AB93-6	1,157	0.429	0.420	0.008
	CONVENTIONAL	CF-CC-BB9-1	800	0.303	0.290
CF-CC-BB9-2		1,087	0.422	0.402	0.019
CF-CC-AB93-1		1,011	0.377	0.368	0.008
CF-CC-AB93-2		1,188	0.446	0.432	0.013

^a Specific surface area calculated by the BET method.

^b Total pore volume recorded at 100 nm on cumulative pore volume by NLDFT carbon slit pore model.

^c Micropore volume obtained at 2 nm on cumulative pore volume by NLDFT carbon slit pore model.

^d Mesoporous volume obtained at 2-50 nm on cumulative pore volume by NLDFT carbon slit pore model.

Table 4. Textural parameters of virgin and regenerated charcoal-derived carbon by microwave and conventional heating

	Sample	^a S _{BET} (m ² /g)	^b V _t (cm ³ /g)	^c V _{micro} (cm ³ /g)	^d V _{mes} (cm ³ /g)	
MICROWAVE	Ch virgin	1,023	0.471	0.358	0.111	
	MW-Ch-BB9-1	659	0.308	0.233	0.072	
	MW-Ch-BB9-2	681	0.313	0.243	0.067	
	MW-Ch-BB9-3	722	0.332	0.257	0.073	
	MW-Ch-BB9-4	728	0.328	0.262	0.063	
	MW-Ch-BB9-5	733	0.346	0.255	0.089	
	MW-Ch-BB9-6	738	0.331	0.266	0.063	
	MW-Ch-AB93-1	884	0.393	0.319	0.072	
	MW-Ch-AB93-2	953	0.416	0.346	0.068	
	MW-Ch-AB93-3	953	0.420	0.344	0.074	
	MW-Ch-AB93-4	965	0.429	0.347	0.080	
	MW-Ch-AB93-5	972	0.451	0.340	0.109	
	MW-Ch-AB93-6	930	0.403	0.338	0.062	
	CONVENTIONAL	CF-Ch-BB9-1	622	0.288	0.222	0.064
		CF-Ch-BB9-2	790	0.369	0.278	0.089
		CF-Ch-AB93-1	899	0.405	0.324	0.078
CF-Ch-AB93-2		992	0.442	0.358	0.082	

^a Specific surface area calculated by the BET method.

^b Total pore volume recorded at 100 nm on cumulative pore volume by NLDFT carbon slit pore model.

^c Micropore volume obtained at 2 nm on cumulative pore volume by NLDFT carbon slit pore model.

^d Mesoporous volume obtained at 2-50 nm on cumulative pore volume by NLDFT carbon slit pore model.

Table 5. Results of data modelling of adsorption isotherms for BB9 and AB93 on virgin and regenerated coconut carbon samples by microwave and conventional heating.

Sample	Langmuir Parameters of model					Freundlich Parameters of model				
	B	Q _M	F _{obj}	R ²	E _{abs} (%)	K	N	F _{obj}	R ²	E _{abs} (%)
CC-BB9	0.2376	212.2	1.059	0.8297	22.11±38.45	113.00	9.936	1.028	0.8470	21.89±38.53
MW-CC-BB9-4	0.0727	127.6	0.095	0.8045	10.86±6.89	29.89	4.358	0.007	0.9900	2.69±2.11
CF-CC-BB9-2	0.0294	213.4	1.020	0.8532	20.93±6.89	63.09	5.511	1.002	0.8854	18.13±40.12
CC-AB93	0.0007	393.7	0.596	0.9175	22.41±24.27	2.70	1.724	0.277	0.8365	20.06±8.46
MW-CC-AB93-4	0.0018	200.8	0.449	0.7779	24.81±12.60	2.38	1.707	0.165	0.8537	16.07±4.50
CF-CC-AB93-2	0.0008	331.3	0.047	0.9859	6.78±6.16	0.61	1.254	0.065	0.9682	8.04±7.18

Table 6. Results of data modelling of adsorption isotherms for BB9 and AB93 on virgin and regenerated charcoal carbon samples by microwave and conventional heating.

Sample	Langmuir	Freundlich
--------	----------	------------

	Parameters of model					Parameters of model				
	B	Q _M	F _{obj}	R ²	E _{abs} (%)	K	N	F _{obj}	R ²	E _{abs} (%)
Ch-BB9	0.0581	246.4	1.007	0.9084	19.32 ±39.56	94.61	6.955	1.035	0.8644	22.45±38.28
MW-Ch-BB9-4	0.0223	155.9	0.038	0.9246	7.07 ±3.95	19.22	3.180	0.049	0.9503	7.65±5.22
CF-Ch-BB9-2	0.0235	181.8	1.040	0.7590	22.68 ±38.24	51.28	5.374	1.010	0.9023	19.73±39.41
Ch-AB93	0.0027	159.8	0.298	0.5307	15.57±17.46	1.69	1.603	0.363	0.6046	22.45±10.98
MW-Ch-AB93-4	0.0020	210.3	0.426	0.6590	21.33±17.46	1.69	1.524	0.234	0.7864	15.25±13.72
CF-Ch-AB93-2	0.0001	1419.2	0.868	0.4940	34.14±18.32	0.02	0.789	0.272	0.8855	17.96±12.55

Table 7. Textural parameters of microwave regenerated samples after several cycles of regeneration

Sample	Cycle	S_{BET} (m^2/g)	V_t (cm^3/g)	V_{micro} (cm^3/g)	V_{mes} (cm^3/g)	% micro	% meso
MW-CC-BB9-4	CC virgin	1,131	0.431	0.417	0.013	96.8	3.0
	Cycle 1	939	0.364	0.346	0.017	94.9	4.8
	Cycle 2	802	0.318	0.301	0.016	94.7	4.9
	Cycle 3	792	0.305	0.289	0.015	94.8	4.8
	Cycle 4	765	0.295	0.280	0.014	94.8	4.8
MW-CC-AB93-4	CC virgin	1,131	0.431	0.417	0.013	96.8	3.0
	Cycle 1	1,140	0.439	0.422	0.015	96.2	3.5
	Cycle 2	1,160	0.450	0.430	0.018	95.8	3.9
	Cycle 3	1,155	0.445	0.427	0.016	96.0	3.7
	Cycle 4	1,088	0.418	0.400	0.017	95.7	4.0
MW-Ch-BB9-5	Ch virgin	1,023	0.471	0.358	0.111	76.0	23.5
	Cycle 1	733	0.346	0.255	0.089	73.8	25.6
	Cycle 2	610	0.286	0.216	0.068	75.5	23.8
	Cycle 3	564	0.267	0.198	0.066	74.5	24.7
	Cycle 4	513	0.239	0.185	0.053	77.2	22.0
MW-Ch-AB93-5	Ch virgin	1,023	0.471	0.358	0.111	76.0	23.5
	Cycle 1	972	0.451	0.340	0.109	75.4	24.1
	Cycle 2	955	0.443	0.336	0.104	75.9	23.5
	Cycle 3	873	0.389	0.312	0.076	80.0	19.5
	Cycle 4	856	0.388	0.306	0.080	78.7	20.6

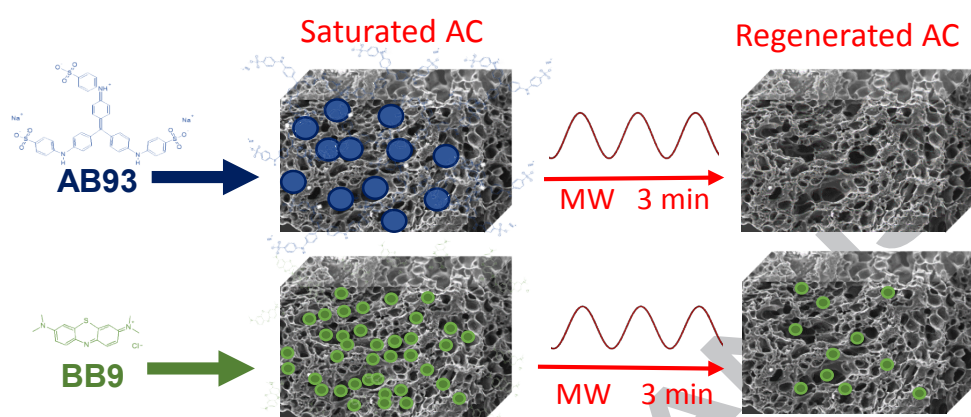
^a Specific surface area calculated by the BET method.

^b Total pore volume recorded at 100 nm on cumulative pore volume by NLDFT carbon slit pore model.

^c Micropore volume obtained at 2 nm on cumulative pore volume by NLDFT carbon slit pore model.

^d Mesoporous volume obtained at 2-50 nm on cumulative pore volume by NLDFT carbon slit pore model.

Graphical abstract



Highlights

► Regeneration of activated carbons loaded with textile dyes ► Dielectric and thermal properties were used to study the selective heating by microwaves ► Comparative study with conventional regeneration ► Adsorption isotherms and modelling of virgin and regenerated activated carbons ► Textural properties and adsorption-regeneration cycles